Design, fabrication and characterization of PC, COP and PMMA-cladded As_2Se_3 microwires

Lizhu Li,* Alaa Al-Kadry, Nurmemet Abdukerim, and Martin Rochette

Department of Electrical and Computer Engineering, 3480 University Street, McGill University, Montréal, H3A 0E9, Canada

lizhu.li@mail.mcgill.ca

Abstract: We introduce the PC- and COP-cladded As_2Se_3 microwires, two highly nonlinear microwires optimized to operate in the wavelength range of 1.85 μm to 2.20 μm. Like the previously reported PMMA-cladded As_2Se_3 microwire, the PC- and COP-cladded microwires benefit of a large waveguide nonlinear parameter and engineerable chromatic dispersion level, but without the absorption features of PMMA in the 1.85 μm to 2.20 μm range. The design rules and fabrication technique of each polymer-cladded microwire is provided. COP- and PMMA-cladded microwires with identical length and waveguide nonlinearity parameter are also operated in the nonlinear regime, highlighting features of self-phase modulation, four-wave mixing and Raman scattering in the 1.85 μm to 2.20 μm range.

OCIS codes: (160.4330) Nonlinear optical materials; (160.4760) Optical properties; (160.5470) Polymers; (220.0220) Optical design and fabrication; (290.5890) Scattering, stimulated; (350.3850) Materials processing.

References and links

1. C. Faust, *Modern Chemical Techniques* (CRC Press, 1995).
2. C. Markos and O. Bang, "Nonlinear label-free biosensing with high sensitivity using As_2S_3 chalcogenide tapered fiber," Opt. Lett. **33**(13), 2892–2898 (2015).
3. B. Pal, *Frontiers in Guided Wave Optics and Optoelectronics* (InTech, 2010)
4. P. F. Moulton, G. A. Rines, E. V. Slobodtchikov, K. F. Wall, G. Frith, B. Samson, and A. L. G. Carter, "Tm-doped fiber lasers: fundamentals and power scaling," IEEE J. Sel. Top. Quantum Electron. **15**(1), 85–92 (2009).
5. C. W. Ruby, M. J. F. Digonnet, and R. L. Byer, "Advances in 2-μm Tm-doped mode-locked fiber lasers," Opt. Fiber Technol. **20**(6), 642–649 (2014).
6. Q. Wang, J. Geng, T. Luo, and S. Jiang, "Mode-locked 2 μm laser with highly thulium-doped silicate fiber," Opt. Lett. **34**(23), 3616–3618 (2009).
7. V. Matsas, T. Newson, D. Richardson, and D. Payne, "Selfstarting passively mode-locked fiber ring soliton laser exploiting nonlinear polarisation rotation," Electron. Lett. **28**(15), 1391–1393 (1992).
8. R. H. Stolen, J. Botineau, and A. Ashkin, "Intensity discrimination of optical pulses with birefringent fibers," Opt. Lett. **7**(10), 512–514 (1982).
9. R. H. Stolen, "Fiber Raman lasers," Fiber Integr. Opt. **3**(1), 21–51 (1980).
10. K. Inoue and H. Toba, "Wavelength conversion experiment using fiber four-wave mixing," IEEE Photonics Technol. Lett. **4**(1), 69–72 (1992).
11. K. A. Rauschenbach, K. L. Hall, J. C. Livas, and G. Raybon, "All-optical pulse width and wavelength conversion at 10 Gb/s using a nonlinear optical loop mirror," IEEE Photonics Technol. Lett. **6**(9), 1130–1132 (1994).
12. D. D. Hudson, S. A. Dekker, E. C. Mägi, A. C. Judge, S. D. Jackson, E. Li, J. S. Sanghera, L. B. Shaw, I. D. Aggarwal, and B. J. Eggleton, "Octave spanning supercontinuum in an As_2S_3 taper using ultralow pump pulse energy," Opt. Lett. **36**(7), 1122–1124 (2011).
13. J. C. Knight, "Photonic crystal fibres," Nature **424**(6950), 847–851 (2003).
14. G. Lenz, J. Zimmermann, T. Katsufuji, M. E. Lines, H. Y. Hwang, S. Spälter, R. E. Slusher, S. W. Cheong, J. S. Sanghera, and I. D. Aggarwal, "Large Kerr effect in bulk Se-based chalcogenide glasses," Opt. Lett. **25**(4), 254–256 (2000).
15. Amorphous materials, Inc., "AMTIR-2: Arsenic selenide glass AsSe," *http://www.amorphousmaterials.com/products/*.
16. Amorphous materials, Inc., "AMTIR-6: Arsenic trisulfide glass As_2S_3," *http://www.amorphousmaterials.com/products/*.
17. V. Ta'eed, N. J. Baker, L. Fu, K. Finsterbusch, M. R. E. Lamont, D. J. Moss, H. C. Nguyen, B. J. Eggleton, D. Y. Choi, S. Madden, and B. Luther-Davies, "Ultrafast all-optical chalcogenide glass photonic circuits," Opt. Express **15**(15), 9205–9221 (2007).

#256224 Received 22 Dec 2015; revised 13 Feb 2016; accepted 16 Feb 2016; published 25 Feb 2016

18. A. Al-kadry, C. Baker, M. El Amraoui, Y. Messaddeq, and M. Rochette, "Broadband supercontinuum generation in As_2Se_3 chalcogenide wires by avoiding the two-photon absorption effects," Opt. Lett. **38**(7), 1185–1187 (2013).
19. E. C. Mägi, L. B. Fu, H. C. Nguyen, M. R. E. Lamont, D. I. Yeom, and B. J. Eggleton, "Enhanced Kerr nonlinearity in sub-wavelength diameter As_2Se_3 chalcogenide fiber tapers," Opt. Express **15**(16), 10324–10329 (2007).
20. C. Baker and M. Rochette, "High nonlinearity and single-mode transmission in tapered multimode-PMMA fibers," IEEE Photonics J. **4**(3), 960–969 (2012).
21. C. Baker and M. Rochette, "Highly nonlinear hybrid AsSe-PMMA microtapers," Opt. Express **18**(12), 12391–12398 (2010).
22. R. Ahmad and M. Rochette, "Chalcogenide optical parametric oscillator," Opt. Express **20**(9), 10095–10099 (2012).
23. R. Ahmad and M. Rochette, "Raman lasing in a chalcogenide microwire-based Fabry-Perot cavity," Opt. Lett. **37**(21), 4549–4551 (2012).
24. R. Ahmad and M. Rochette, "High efficiency and ultra broadband optical parametric four-wave mixing in chalcogenide-PMMA hybrid microwires," Opt. Express **20**(9), 9572–9580 (2012).
25. R. Ahmad and M. Rochette, "All-chalcogenide Raman-parametric laser, wavelength converter, and amplifier in a single microwire," IEEE J. Sel. Top. Quantum Electron. **20**(5), 299–304 (2014).
26. A. Al-Kadry, L. Li, M. El Amraoui, T. North, Y. Messaddeq, and M. Rochette, "Broadband supercontinuum generation in all-normal dispersion chalcogenide microwires," Opt. Lett. **40**(20), 4687–4690 (2015).
27. A. Al-Kadry, M. El Amraoui, Y. Messaddeq, and M. Rochette, "Mode-locked fiber laser based on chalcogenide microwires," Opt. Lett. **40**(18), 4309–4312 (2015).
28. J. C. Beugnot, R. Ahmad, M. Rochette, V. Laude, H. Maillotte, and T. Sylvestre, "Reduction and control of stimulated Brillouin scattering in polymer-coated chalcogenide optical microwires," Opt. Lett. **39**(3), 482–485 (2014).
29. A. Dot, E. Meyer-Scott, R. Ahmad, M. Rochette, and T. Jennewein, "Converting one photon into two via four-wave mixing in optical fibers," Phys. Rev. A **90**(4), 043808 (2014).
30. E. Meyer-Scott, A. Dot, R. Ahmad, L. Li, M. Rochette, and T. Jennewein, "Power-efficient production of photon pairs in a tapered chalcogenide microwire," Appl. Phys. Lett. **106**(8), 081111 (2015).
31. J. Málek and J. Shánělová, "Structural relaxation of As_2Se_3 glass and viscosity of supercooled liquid," J. Non-Cryst. Solids **351**(43-45), 3458–3467 (2005).
32. D. W. Henderson and D. G. Ast, "Viscosity and crystallization kinetics of As_2Se_3," J. Non-Cryst. Solids **64**(1–2), 43–70 (1984).
33. A. S. Tverjanovich, "Temperature dependence of the viscosity of chalcogenide glass-forming melts," Glass Phys. Chem. **29**(6), 532–536 (2003).
34. T. Tofteber and E. Andreassen, "Injection moulding of microfeatured parts," Proceedings of the Polymer Processing Society 24th Annual Meeting (2008).
35. P. Lomellini, "Viscosity-temperature relationships of a polycarbonate melt: Williams-Landel-Ferry versus Arrhenius behavior," Makromol. Chem. **193**(1), 69–79 (1992).
36. C. Liu, J. He, R. Keunings, and C. Bailly, "New linearized relation for the universal viscosity-temperature behavior of polymer melts," Macromolecules **39**(25), 8867–8869 (2006).
37. W. Martienssen and H. Warlimont, *Springer Handbook of Condensed Matter and Materials Data* (Springer Science & Business Media, 2006)
38. X. Lin, A. Kelly, D. Ren, M. Woodhead, P. Coates, and K. Wang, "Geometrical dependence of viscosity of polymethylmethacrylate melt in capillary flow," J. Appl. Polym. Sci. **130**(5), 3384–3394 (2013).
39. W. Fred and J. R. Billmeyer, *Textbook of Polymer Science* (John Wiley and Sons, 1984).
40. J. E. Mark, *Physical Properties of Polymers Handbook* (AIP Press, 1996).
41. L. P. Zeon Chemicals, "The lowest autofluorescent injection-moldable plastic," *http://www.zeonex.com/life-sciences.aspx*.
42. M. N. Eakins, "New plastics for old vials," Bioprocess Int. **3**, 52–58 (2005).
43. J. Nishii, T. Yamashita, and T. Yamagishi, "Chalcogenide glass fiber with a core-cladding structure," Appl. Opt. **28**(23), 5122–5127 (1989).
44. G. P. Agrawal, *Nonlinear Fiber Optics* (Academic, 2007).
45. G.-S. Plastic Optics, "Transmission curves," *http://www.gsoptics.com/transmission-curves/*.

1. Introduction

The wavelength range of 2 μm is of broad interest for LIDAR, gas sensing systems, free-space communications and medical applications [1–3]. Semiconductor lasers and Thulium-doped fibers provide gain in the wavelength range of 2 μm, thus providing access to compact laser sources [4–6]. The operation of a 2 μm laser depends on the availability of a variety of components compatible with this wavelength range. Of most importance, a nonlinear medium enables the laser to be operated in a pulsed regime [7,8]. As well as it could be used for wavelength conversion [9–11].

Compact and highly nonlinear media compatible with the wavelength range of 2 μm include high modal confinement waveguides such as optical fiber microwires and photonic

#256224 Received 22 Dec 2015; revised 13 Feb 2016; accepted 16 Feb 2016; published 25 Feb 2016

crystal fibers [12,13]. The large intrinsic nonlinearity (n_2) and transparency are the two most important properties that a material must have to serve as a compact nonlinear medium. Chalcogenide glasses are excellent candidates to play this role because their n_2 is up to a factor of 1000 times larger than for the widespread silica glass [14]. Moreover, the transparency spectrum of chalcogenide glasses is ideal for applications over a broad wavelength range: Arsenic selenide (As_2Se_3) transmits light from 1 to 12 μm [15], and Arsenic sulfide (As_2S_3) transmits light from 1 to 8 μm [16]. Chalcogenide glasses also have negligible two-photon absorption and free carrier absorption in the 2 μm wavelength range [17,18].

In its simplest form, the waveguide structure of the chalcogenide microwire consists of a chalcogenide core surrounded by a cladding of ambient air [19]. With a wire diameter in the order of the wavelength, the air-cladding chalcogenide microwire unfortunately has a limited usefulness because of its extreme mechanical fragility and quick degradation when exposed to dust of a non-controlled environment. In order to overcome these limitations, Baker et al. have successfully fabricated the first polymer-cladded chalcogenide microwire [20,21], which consists of a chalcogenide microwire coated with PolyMethyl MethAcrylate (PMMA) [21]. The PMMA cladding provides mechanical strength to the chalcogenide microwire and protects it from environmental contamination and degradation. Being now a practical component, the hybrid PMMA/chalcogenide microwire has been used for several applications at telecommunication wavelengths: Optical amplification and laser oscillation based on Raman and parametric gains [22–24], wavelength conversion [25], supercontinuum generation [26], they have served as nonlinear engines in a self-pulsating fiber laser cavity [27] and served to reduce and control stimulated Brioullin scattering [28]. For quantum cryptography, the hybrid chalcogenide microwires have been used to convert one photon into two [29] as well as producing photon pairs with unprecedented efficiency [30].

Despite the many successful demonstrations of the PMMA/chalcogenide microwire, the limited transparency of PMMA at wavelengths beyond 1.55 μm is non-negligible and attenuates the propagating signal. This attenuation comes from the evanescent coupling of light from the chalcogenide core to the PMMA cladding, and is characteristic of microwires of several centimeters long.

In this paper, we investigate the use of alternative polymers to coat the As_2Se_3 microwire with a goal to operate them in the 1.85 μm to 2.20 μm wavelength range. The cladding compositions under study include PolyCarbonate (PC), Cyclo Olefin Polymer (COP) 480R, COP 1020R, and PMMA as the reference polymer.

2. Hybrid microwires fabrication

Several factors must be considered in the design and fabrication of hybrid microwires to ensure that the As_2Se_3 glass and the polymer cladding are, as much as possible, compatible optically and mechanically. These factors include: (1) the transmission wavelength range of the cladding material; (2) the refractive index of the cladding material, as shown in Table 1; (3) the glass transition temperature (T_g) of As_2Se_3 glass and polymer, as shown in Table 1; and (4) the temperature-dependent viscosity of As_2Se_3 glass and polymer. Figure 1 shows the logarithmic plot of viscosity of As_2Se_3 [31–33], PC [34,35], COP [36] and PMMA [37,38] at different temperatures. For a hybrid microwire to operate at wavelengths beyond 1.85 μm, the chosen cladding material must be relatively low-loss at the target transmission wavelength. The refractive index of the cladding material should also be as low as possible, below the refractive index of As_2Se_3, to ensure the optical mode is strongly confined in the As_2Se_3 material, and thus limiting the penetration depth of the evanescent wave in the polymer. Mechanically, the As_2Se_3 and cladding material must be compatible by sharing close values of T_g, as shown in Table 1, and viscosity, as shown in Fig. 1, to ensure they can be heated and stretched together from a hybrid preform, to a hybrid fiber, and finally to a hybrid microwire [20].

#256224 Received 22 Dec 2015; revised 13 Feb 2016; accepted 16 Feb 2016; published 25 Feb 2016

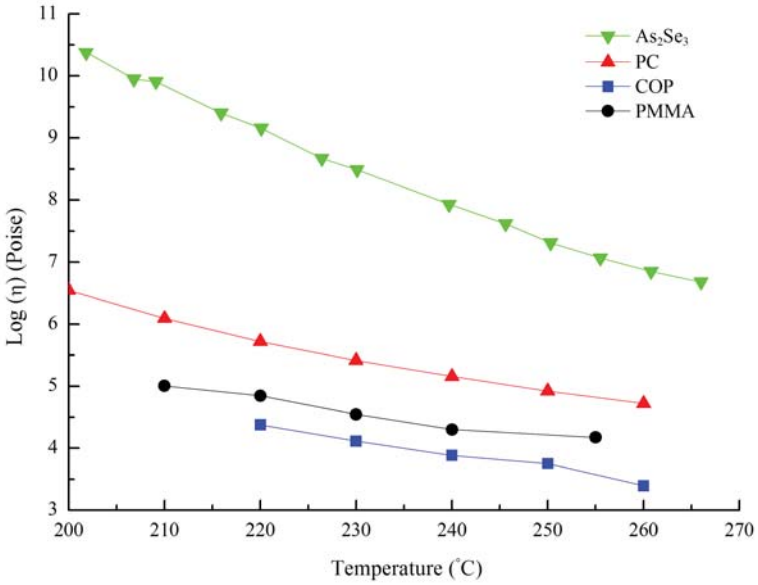

Fig. 1. Logarithmic plot of viscosity of As_2Se_3, PC, COP and PMMA at different temperatures.

Table 1. Glass transition temperature and refractive index at 1.94 µm of chalcogenide and polymers

	Glass transition temperature T_g (°C)	Calculated refractive index
As_2Se_3	167 [15]	2.81
PMMA	105 [39]	1.47
PC	150 [40]	1.56
COP 480R	138 [41]	1.51
COP 1020R	105 [42]	1.49

PC and COP are good candidates to replace PMMA because they provide an improved optical transmission beyond 1.85 µm with respect to PMMA, as well as being mechanically compatible with As_2Se_3. Figure 2(a) shows a schematic of the rod-in-tube method used to fabricate polymer-cladded As_2Se_3 hybrid preform [43]. It consists of a three-layer structure leading to a waveguide with an As_2Se_3 core, a polymer (PC, COP, or PMMA) cladding, and a PMMA coating.

The microwire fabrication is performed in multiple steps. The first step consists in making a hybrid preform, then the hybrid preform is stretched into a hybrid fiber, and finally the hybrid fiber is stretched into a microwire.

Hybrid preform: Fig. 2(a) shows a schematic of the hybrid preform fabrication setup. A cylinder of bulk As_2Se_3 is inserted into a PC or COP capillary tube, and the assembly is inserted into a PMMA tube. The assembly is pushed at a constant feed velocity V_f into a heated funnel. Under heat and pressure, the PMMA tube and the polymer capillary tube collapse together on the As_2Se_3 cylinder in an air-free composite cylinder. The multimaterial composite is extruded at the bottom of the funnel and drawn at a constant speed V_d to obtain a hybrid preform with a uniform diameter. Figure 2(b) shows the photograph of extruded preform.

Hybrid fiber: Figure 2(c) shows a schematic of the hybrid fiber fabrication setup. In a second step, the hybrid preform is heated and stretched to reduce further its diameter down to obtain a hybrid fiber with As_2Se_3 core diameter ϕ_{AsSe}, leading to maximum coupling efficiency with e.g. SMF-28 fiber. A segment of uniform hybrid fiber is cut-off and both ends are

#256224 Received 22 Dec 2015; revised 13 Feb 2016; accepted 16 Feb 2016; published 25 Feb 2016

polished. Figure 2(d) and 2(e) show the reflection optical micrograph of cross section of hybrid fiber with diameter ϕ_{PMMA} = 770.0 µm and As_2Se_3-COP core-cladding with diameter ϕ_{AsSe} = 18.2 µm and ϕ_{COP} = 190.2 µm. The hybrid fiber is designed to be optically compatible with the waveguide that it interfaces e.g. SMF-28, therefore minimizing the insertion and extraction coupling losses.

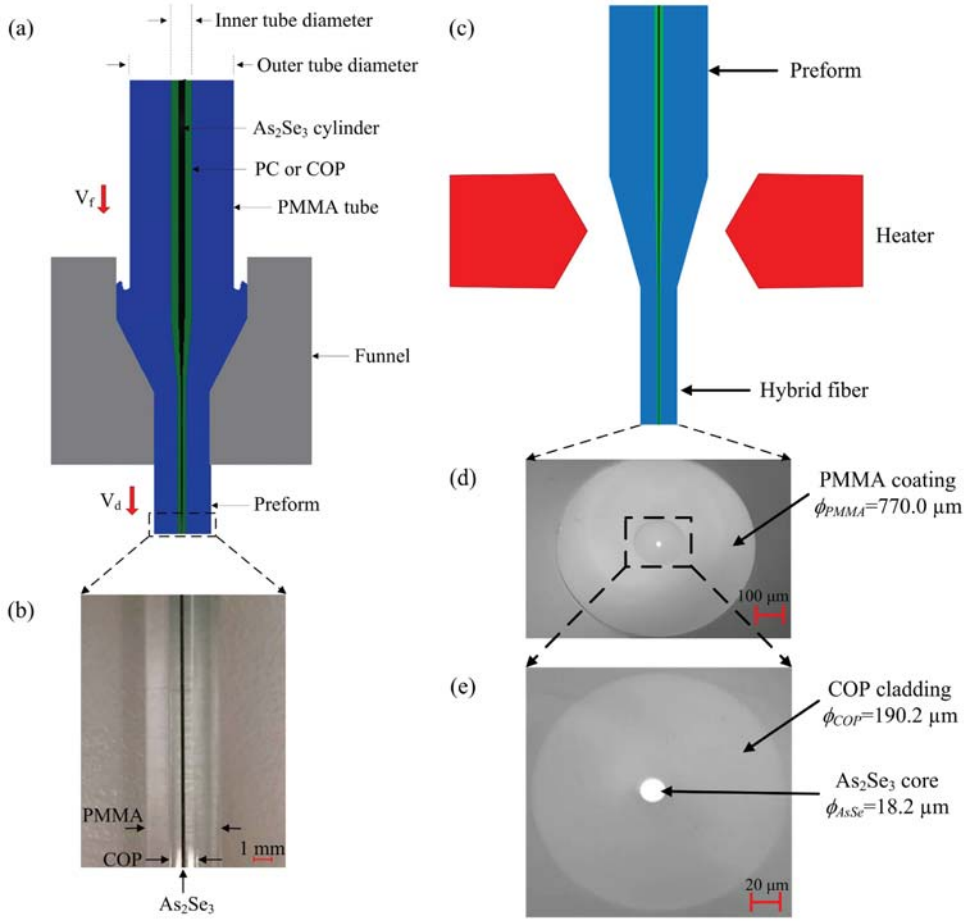

Fig. 2. (a) Schematic of the polymer-cladded As_2Se_3 preform fabrication setup. (b) photograph of extruded preform. (c) schematic of hybrid fiber fabrication setup. (d) reflection optical micrograph of cross section of hybrid fiber. (e) reflection optical micrograph of the As_2Se_3-COP core-cladding.

Hybrid microwire: Finally, the hybrid microwire is fabricated from heating and stretching a sample of the hybrid fiber [20]. Figure 3(a) shows a schematic of polymer-cladded As_2Se_3 microwire fabrication setup. The robust microwire is manually removed from the tapering setup and transferred to a coupling setup; both ends of the microtaper are aligned and permanently butt-coupled to SMF-28 fibers using UV-cured epoxy. Figure 3(b) shows the various sections of a microtaper. The microwire is the thin central section of the microtaper. Figure 3(c) shows the photograph of a microtaper with microwire section length of 10 cm.

#256224 Received 22 Dec 2015; revised 13 Feb 2016; accepted 16 Feb 2016; published 25 Feb 2016

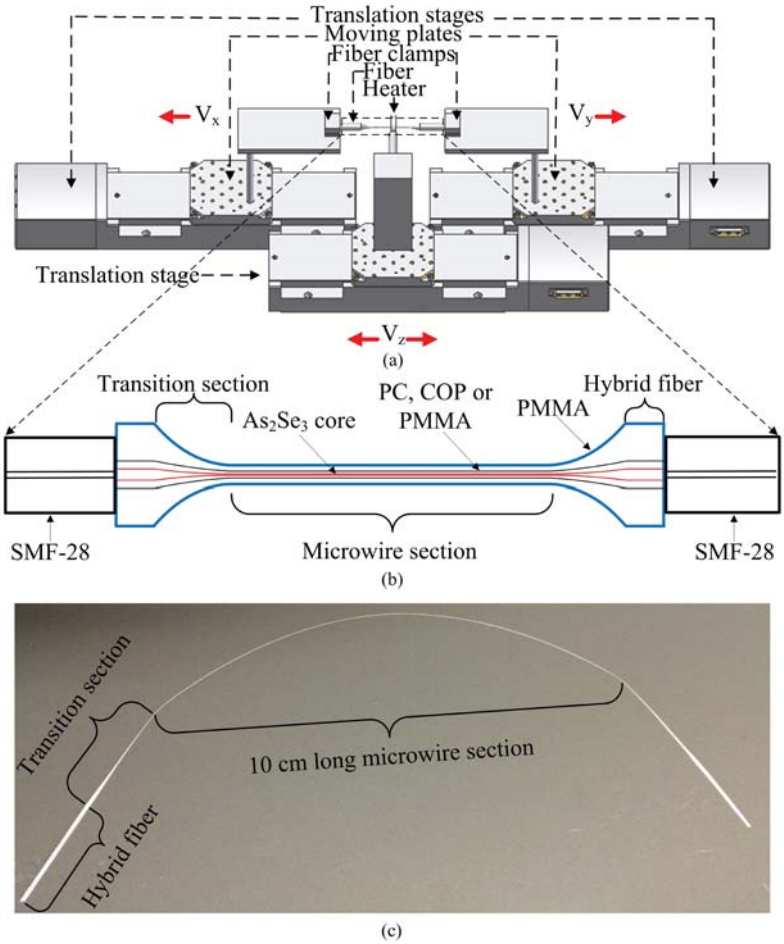

Fig. 3. (a) Schematic of polymer-cladded As_2Se_3 microtaper fabrication setup. (b) schematic of the polymer-cladded As_2Se_3 microtaper coupled to SMF-28 fiber. (c) photograph of a microtaper.

3. Simulation

Chromatic dispersion β_2, waveguide nonlinearity parameter γ, and confinement factor $\Gamma = P_{core}/P_{total}$, where P_{core} is the modal power enclosed in the core and P_{total} is the total mode power, are three fundamental parameters of a microwire. Their values depend on the microwire diameter and materials composition. Solving the characteristic equation of a cylindrical waveguide leads to the propagation constant β and the electric and magnetic fields distribution E and H for the fundamental mode HE_{11} mode, themselves leading to β_2, γ and Γ [44].

Figure 4(a) presents β_2 and γ of the PC-, COP 480R-, and PMMA-cladded As_2Se_3 microwires as a function of core diameter at an operation wavelength of 1.94 μm. Every polymer-cladded microwire has two zero dispersion diameters (ZDD), which are defined as ZDD_1 and ZDD_2 in the order of increasing wire diameter. When the diameter increases, β_2 asymptotically converges towards the value of bulk As_2Se_3. The advantage of a double ZDD microwire is that it enables to select which ZDD should be used based on the application requirements. At ZDD_1, the microwire has high γ, but the slope of β_2 (= β_3) is large, the microwire has relatively low confinement factor, and thus the attenuation caused by the evanescent wave in an absorbing cladding is comparatively high. At ZDD_2, the microwire has

#256224 Received 22 Dec 2015; revised 13 Feb 2016; accepted 16 Feb 2016; published 25 Feb 2016

a slightly reduced γ, but the slope of β_2 is small. As well the confinement factor is higher than at ZDD_1, and thus an absorbing cladding has less impact at ZDD_2 than at ZDD_1.

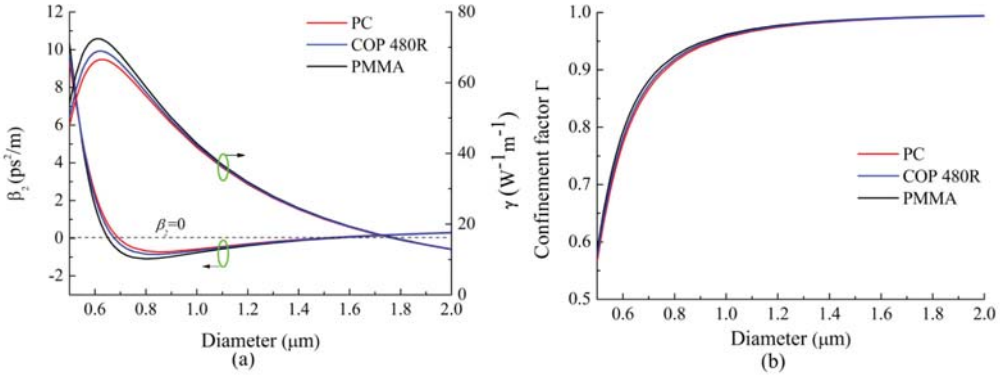

Fig. 4. (a) Chromatic dispersion β_2 and waveguide nonlinearity parameter γ (b) confinement factor Γ of the PC-, COP 480R- and PMMA-cladded microwires as a function of the As_2Se_3 core diameter at an operation wavelength of 1.94 μm.

Figure 4(b) shows the confinement factor of the PC-, COP 480R-, and PMMA-cladded microwires as a function of the As_2Se_3 core diameter at an operation wavelength of 1.94 μm. The mode confinement increases with increasing core diameter. The attenuation coefficient α_{total} resulting from the modal propagation in a waveguide is given by $\alpha_{total} = \alpha_{core} \times \Gamma + \alpha_{clad} \times (1-\Gamma)$, where α_{core} is the attenuation coefficient of the core material, and α_{clad} is the attenuation coefficient of the cladding material. Table 2 summaries β_2, γ and Γ at relevant diameters of As_2Se_3-PMMA, As_2Se_3-PC, and As_2Se_3-COP 480R microwires.

Table 2. Dispersion, nonlinearity and confinement properties of PMMA-, PC-, and COP 480R-cladded microwires at an operation wavelength of 1.94 μm. γ_{max}: maximum γ; $d_{\gamma max}$: diameter corresponding to maximum γ

	PMMA	PC	COP 480R
ZDD_1 (μm)	0.655	0.696	0.602
γ at ZDD_1 ($W^{-1}m^{-1}$)	71.1	64.0	68.7
Γ at ZDD_1	0.847	0.861	0.788
ZDD_2 (μm)	1.549	1.497	1.625
γ at ZDD_2 ($W^{-1}m^{-1}$)	20.5	21.5	18.8
Γ at ZDD_2	0.989	0.986	0.990
γ_{max} ($W^{-1}m^{-1}$)	72.5	66.6	68.9
$d_{\gamma max}$ (μm)	0.616	0.628	0.616
Γ at $d_{\gamma max}$	0.808	0.802	0.806
β_2 at $d_{\gamma max}$ (ps^2/m)	1.16	1.47	–0.490

4. Experimental results

For the experiment, polymer-cladded microwires with PC, COP and PMMA claddings have been designed with a diameter of 1.5 μm and a length of 10 cm. The diameter size has been selected because of the following aspects: This diameter is close to ZDD_2 and thus desirable for practical applications when normal, anomalous or zero dispersion is needed. Secondly, γ is significantly large at this point, thus being useful for nonlinear applications with compact size and low power consumption. Finally and most importantly, we should observe the absorption features of the various polymers via evanescent wave coupling, if there is any, as expected from Γ. As well, the microwire section length of the polymer-cladded microtapers was chosen 10 cm long in order to highlight the absorption features in those microwires. The total absorption of the microwire increases exponentially with increasing length. However take

#256224 Received 22 Dec 2015; revised 13 Feb 2016; accepted 16 Feb 2016; published 25 Feb 2016

note that in many practical applications, a microwire shorter than 10 cm provides enough nonlinearity to be functional, limiting the negative impact of an absorptive cladding [26].

The optical transmission of polymer-cladded As_2Se_3 microwires has been measured in the spectral window in between 1.45 μm and 2.20 μm using a combination of erbium and thulium amplified spontaneous emission (ASE) source, and a Yokogawa AQ6375 optical spectrum analyzer (OSA) at either side of the device under test. PC-, COP 480R-, COP 1020R-, and PMMA-cladded As_2Se_3 microwires with core diameter ϕ_{AsSe} = 1.5 μm and length L_w = 10 cm have been fabricated and tested.

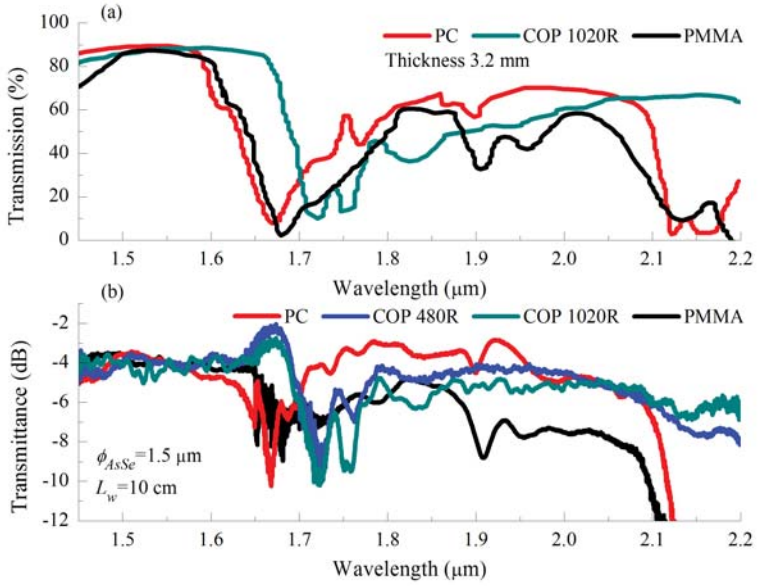

Fig. 5. (a) Transmission spectra of PC, COP 1020R and PMMA. (b) SMF-28 to SMF-28 transmittance of the PC-, COP 480R-, COP 1020R- and PMMA-cladded microwires with diameter ϕ_{AsSe} = 1.5 μm and length L_w = 10 cm.

Figure 5(a) shows the measured transmission spectra of PC [45], COP 1020R [45] and PMMA [45] sheet with the same thickness of 3.2 mm. Figure 5(b) shows the transmission spectrum of each polymer-cladded As_2Se_3 microwire. The typical SMF-28 to SMF-28 insertion loss of the microwires is 4 dB at a wavelength of 1.55 μm. At wavelengths in between 1.85 μm and 2.20 μm, the transmittance spectrum of microwires with PC, COP 480R and COP 1020R claddings is increased with respect to microwires made solely out of PMMA. Especially when the operating wavelength is above 1.9 μm, PC and COP claddings transmit significantly better than PMMA. All of these polymers have absorption peaks around 1.7 μm, caused by the first order overtone of carbon hydrogen (C-H) chemical bonds.

PC- and PMMA-cladded As_2Se_3 microwires transmit light with an abrupt cut at 2.1 μm. COP 480R- and COP 1020R-cladded As_2Se_3 microwires transmit light up to at least 2.2 μm, limited by the experimental transmission measurement. The transmission spectrum of each polymer-cladded As_2Se_3 microwire, as shown in Fig. 5(b), is consistent with the transmission spectrum of bulk polymer, as shown in Fig. 5(a).

Next, we compare the efficiency of nonlinear processes in between a COP 480R-cladded and a PMMA-cladded As_2Se_3 microwires. To get equal waveguide nonlinear parameters, the corresponding core diameters of COP- and PMMA-cladded microwires are 1.49 μm and 1.50 μm, respectively, leading to γ = 21.7 $W^{-1}m^{-1}$ in both cases. As well, pump pulses centered at a wavelength of 1.94 μm and with a duration of 3 ps are being launched into the microwires. The average input power delivered into the microwire section is 1.3 mw, corresponding to a peak pulse power of 14.1 W. The transmission loss of the 10 cm long COP 480R- and PMMA-cladded As_2Se_3 microwires at a wavelength of 1.94 μm is 0.33 dB/cm and

#256224 Received 22 Dec 2015; revised 13 Feb 2016; accepted 16 Feb 2016; published 25 Feb 2016

0.59 dB/cm, respectively, leading to an effective length L_{eff} = (1-exp(-αL))/α of 7.00 cm and 5.46 cm, respectively.

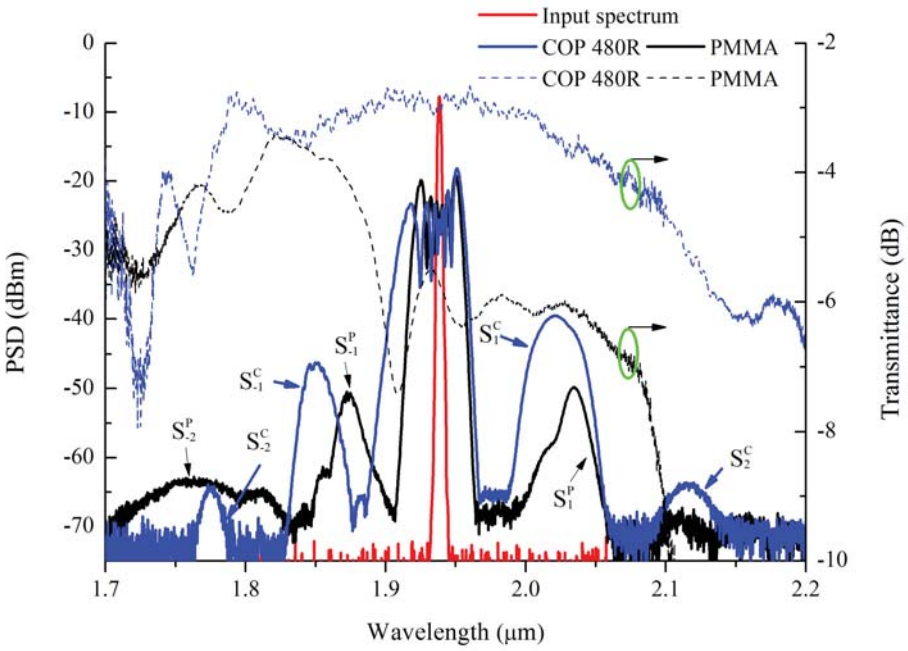

Fig. 6. Nonlinearly broadened spectra of COP 480R- and PMMA-cladded microwires with length L_w = 10 cm and γ = 21.7 $W^{-1}m^{-1}$. The peak pump power is 14.1 W and is centered at a wavelength of 1.94 μm. Transmission spectra are also given for reference

Figure 6 shows the resulting spectrum of COP 480R- and PMMA-cladded microwires pumped by 3 ps pulses centered at a wavelength of 1.94 μm. Transmission spectra are also given for reference. As the peak pump power is increased up to 14.1 W, nonlinear scattering bands are observed along with spectral broadening of the pump signal. For COP 480R- and PMMA-cladded As_2Se_3 microwires, the theoretical nonlinear phase shift $\phi_{NL}=\gamma P_0 L_{eff}$ is 6.82π and 5.32π, respectively, which agrees well with the measured nonlinear phase shift ϕ_{NL} extracted from spectra in Fig. 6. Taking the pump wavelength as a reference, the nonlinear scattering towards longer wavelengths includes Raman scattering and four-wave mixing; the nonlinear scattering in the shorter wavelength direction includes only four-wave mixing. $S_{\pm n}^{m}$ means n_{th} order nonlinear scattering, +/- signs stand for a nonlinear scattering at longer/shorter wavelengths with respect to the pump. The superscript m designates the cladding material of the microwire (p for PMMA, c for COP 480R). The peak value of S_1^c is 10.3 dB higher than that value of S_1^p shown in Fig. 6 since the transmission loss of COP 480R-cladded As_2Se_3 microwire is more than 2.5 dB lower than that value of PMMA-cladded As_2Se_3 microwire at the corresponding wavelength. Also, the bandwidth of S_1^c is 16 nm wider than that value of S_1^p. With same pump peak power of 14.1 W, COP 480R-cladded As_2Se_3 microwire has second order nonlinear scattering S_2^c in longer wavelength direction. In contrast, PMMA-cladded As_2Se_3 microwire does not have second order nonlinear scattering since the transmission loss of PMMA-cladded As_2Se_3 microwire is more than 6 dB larger than that value of COP 480R-cladded As_2Se_3 microwire above 2.1 μm. The peak value of S_{-1}^c is 4.3 dB higher than that value of S_{-1}^p. The bandwidth of S_{-1}^c is 4.9 nm wider than that value of S_{-1}^p. The peak value of S_{-2}^c is slightly lower than that value of S_{-2}^p. Also, the bandwidth of S_{-2}^c is narrower than that value of S_{-2}^p since COP has two absorption peaks located at 1.73 μm and 1.76 μm, which increase the transmission loss, and reduce the nonlinear scattering.

#256224 Received 22 Dec 2015; revised 13 Feb 2016; accepted 16 Feb 2016; published 25 Feb 2016

5. Conclusion

In summary, PC-, COP 480R-, COP 1020R-, and PMMA-cladded As_2Se_3 microwires have been designed, fabricated and characterized. Microwires with PC cladding have better transmission than that with PMMA cladding at wavelengths from 1.85 μm to 2.10 μm. Microwires with COP 480R cladding have better transmission than that with PMMA cladding at wavelengths from 1.85 μm to 2.20 μm. Due to the strong absorption of C-H bonds, the transmission of PC-cladded As_2Se_3 microwires with length of 10 cm is limited to an upper bound of 2.12 μm. The COP 480R- and COP 1020R-cladded As_2Se_3 microwires with length of 10 cm transmit light up to at least 2.20 μm. The transmission window of these microwires can be further extended by reducing the wire length. Compared with PMMA-cladded microwires, COP 480R-cladded microwires provide an increased nonlinear gain and wider gain bandwidth from 1.85 μm to 2.20 μm.

Acknowledgment

The authors are thankful to Coractive High-Tech for providing the chalcogenide glass used in the experiments, and the Collaborative Research and Development Program of the Natural Sciences and Engineering Research Council of Canada (NSERC).

#256224 Received 22 Dec 2015; revised 13 Feb 2016; accepted 16 Feb 2016; published 25 Feb 2016